Cluster synchronization of starlike networks with normalized Laplacian coupling: master stability function approach

Pavel V. Kuptsov[a] and Anna V. Kuptsova[a]

[a]Institute of electronics and mechanical engineering, Yuri Gagarin State Technical University of Saratov, Politekhnicheskaya 77, Saratov 410054, Russia

ABSTRACT

A generalized model of starlike network is suggested that takes into account non-additive coupling and nonlinear transformation of coupling variables. For this model a method of analysis of synchronized cluster stability is developed. Using this method three starlike networks based on Ikeda, predator-prey and Hénon maps are studied.

Keywords: starlike network, master stability function, cluster synchronization, full chaotic synchronization

1. INTRODUCTION

In this paper we consider starlike networks that consist of a single hub node connected with all other nodes, and subordinate nodes that have only one connection with the hub and are not connected with each other.

The starlike networks is an interesting object of study due to the following reasons. First, they are the simplest and regular representatives of so called scale-free networks that attract a lot of interest now as models for a large variety of natural systems.[1,2] These networks are "scale-free" since their node degree distributions have power law shapes. As a result a small number of nodes hold a major balk of links while the rest of nodes have few connections.[3] Another reason for interest to starlike networks is that their dynamics is amazingly rich. The main their feature is multistability when the number of attractors is very high, and their basins have fractal boundaries that are highly interwoven. It is known that in this case the dynamics is very sensible to the initial state: even tiny perturbation results in arriving at new regime. Moreover, the ranges of existence of particular attractors can be narrow so that the qualitative behavior of the system can change dramatically when its parameters are slightly varied.[4–6]

In the present paper we suggest a generalized model of starlike network taking into account non-additive coupling and nonlinear transformation of coupling variables. For this model we develop an analysis of stability of synchronized clusters generalizing the idea of master stability function.[7] Using this method we study the dynamics of three starlike networks based on Ikeda, predator-prey and Hénon maps.

2. GENERIC MODEL

We are going to consider dynamical networks of N elements with nodes occupied by M dimensional identical discrete time systems:

$$x_n^{(m)}(t+1) = f^{(m)}[\overrightarrow{x}_n(t), h_n^{(m)}(t)], \tag{1}$$

$$h_n^{(m)}(t) = \epsilon_m \sum_{j=1}^{N} \ell_{nj} g^{(m)}[\overrightarrow{x}_j(t)]. \tag{2}$$

Here upper indexes $m = 1, \ldots, M$ enumerate local variables of maps, and lower ones $n = 1, \ldots, N$ runs along network nodes. Functions $f^{(m)}(\overrightarrow{x}, h)$ determine a node map, where vector $\overrightarrow{x} = (x^{(1)}, \ldots, x^{(M)})^{\mathrm{T}}$ is a shorthand for its M arguments, and h is its $(M+1)$th argument responsible for the coupling. Function $g^{(m)}(\overrightarrow{x})$ depends
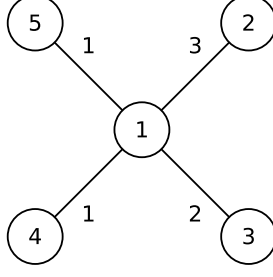
Figure 1. Starlike network with $N = 5$ nodes. Links have positive integer weights.

on M arguments and defines nonlinear transformation of coupling variables. The network structure is given by a $N \times N$ matrix $\mathbf{L} = \{\ell_{nj}\}$. Its particular structure will be specified below. Finally, the coupling strength is controlled by ϵ_m.

Any stability analysis requires Jacobian matrix and corresponding equation for infinitesimal perturbations to a trajectory. Differentiating $x_n^{(m)}(t+1)$ by $x_k^{(i)}(t)$ one obtains:

$$\delta x_n^{(m)}(t+1) = \sum_{i=1}^{M} \sum_{k=1}^{N} \left(\delta_{nk} f_{in}^{(m)} + f_{M+1,n}^{(m)} \epsilon_m \ell_{nk} g_{ik}^{(m)} \right) \delta x_k^{(i)}(t) \tag{3}$$

where $\delta x_n^{(m)}(t)$ is a perturbation to mth variable of nth node, and

$$f_{in}^{(m)} \equiv \frac{\partial}{\partial x^{(i)}} f^{(m)}(\vec{x}_n, h_n^{(m)}), \quad f_{M+1,n}^{(m)} \equiv \frac{\partial}{\partial h} f^{(m)}(\vec{x}_n, h_n^{(m)}), \quad g_{ik}^{(m)} \equiv \frac{\partial}{\partial x^{(i)}} g^{(m)}(\vec{x}_k). \tag{4}$$

Grouping perturbations to variables with identical indexes into N dimensional vectors $\vec{\delta x}^{(m)} = (\delta x_1^{(m)}, \dots, \delta x_N^{(m)})^{\mathrm{T}}$ one can rewrite Eq. (3) as

$$\vec{\delta x}^{(m)}(t+1) = \sum_{i=1}^{M} \mathbf{B}_{mi} \vec{\delta x}^{(i)}(t) \tag{5}$$

where

$$\mathbf{B}_{mi} = \mathbf{F}_{mi} + \epsilon_m \mathbf{\Phi}_m \mathbf{L} \mathbf{G}_{mi} \tag{6}$$

and

$$\mathbf{F}_{mi} = \operatorname{diag}\{f_{in}^{(m)}, n = 1, \dots, N\}$$
$$\mathbf{\Phi}_m = \operatorname{diag}\{f_{M+1,n}^{(m)}, n = 1, \dots, N\} \tag{7}$$
$$\mathbf{G}_{mi} = \operatorname{diag}\{g_{in}^{(m)}, n = 1, \dots, N\}$$

Thus, the Jacobian matrix of the network (1) is $M \times M$ block matrix whose cells are $N \times N$ matrices $\mathbf{B}_{mi}$

3. STARLIKE NETWORKS

Starlike networks that we consider in this paper has a single hub node and some number of subordinate ones. Each subordinate is connected with the hub and no subordinates are connected with each other. Each connection can have integer positive weight. An example of the star with $N = 5$ nodes is shown in Fig. 1. The weights of links will be denoted as w_i, where $i = 2, \dots, N$ is an index of the corresponding subordinate node. In Fig. 1 $w_2 = 3$, $w_3 = 2$, $w_4 = 1$, and $w_5 = 1$.

The adjacency matrix of a starlike network can be written as

$$\mathbf{A} = \begin{pmatrix} 0 & \mathbf{w} \\ \mathbf{w}^{\mathrm{T}} & \{\mathbf{0}\}_2^N \end{pmatrix}, \tag{8}$$

where $\mathbf{w} = (w_2, w_3, \ldots, w_N)$ and $\{\mathbf{0}\}_2^N$ is $N - 1 \times N - 1$ matrix of zeros. Let $\mathbf{K}$ be a diagonal matrix of row sums of $\mathbf{A}$. The normalized Laplacian coupling matrix reads:

$$\mathbf{L} = \mathbf{K}^{-1}\mathbf{A} - \mathbf{I}. \tag{9}$$

We already considered this type of coupling matrices for scale-free and starlike networks of Hénon maps.[6,8]

Substituting this $\mathbf{L}$ to equation for a cell $\mathbf{B}_{mi}$ of the Jacobian matrix (6) one gets:

$$\mathbf{B}_{mi} = \begin{pmatrix} \{\mathbf{F}_{mi}\}_1^1 - \epsilon_m \{\mathbf{G}_{mi}\}_1^1 \{\mathbf{\Phi}_{mi}\}_1^1 & \epsilon_m \{\mathbf{\Phi}_{mi}\}_1^1 \mathbf{w} \{\mathbf{G}_{mi}\}_2^N / W \\ \epsilon_m \{\mathbf{G}_{mi}\}_1^1 \{\mathbf{\Phi}_{mi}\}_2^N \mathbf{d}^{\mathrm{T}} & \{\mathbf{F}_{mi}\}_2^N - \epsilon_m \{\mathbf{\Phi}_{mi}\}_2^N \{\mathbf{G}_{mi}\}_2^N \end{pmatrix}, \tag{10}$$

where $\mathbf{d} = (1, 1, \ldots, 1)$, and $W = \sum_{i=2}^N w_i$. Symbol $\{\mathbf{F}\}_i^j$ stands for square diagonal submatrix including elements form ith to jth of the diagonal matrix $\mathbf{F}$, and the same for other matrices.

4. CLUSTER SYNCHRONIZATION AND HIERARCHY OF INVARIANT MANIFOLDS

The normalized Laplacian coupling matrix (9) admits the full synchronization of the whole star when $\vec{x}_1(t) = \cdots = \vec{x}_N(t)$ for any t. Moreover the full synchronization of any number of subordinate nodes is also possible, i.e., cluster synchronization can be observed. To understand why this is the case let us write h_n^m, see Eq. (2), for a starlike network explicitly:

$$h_1^{(m)} = \epsilon_m \left[\sum_{j=2}^N w_j g^{(m)}(\vec{x}_j)/W - g^{(m)}(\vec{x}_1) \right], \tag{11}$$

$$h_n^{(m)} = \epsilon_m \left[g^{(m)}(\vec{x}_1) - g^{(m)}(\vec{x}_n) \right], \ n \geq 2. \tag{12}$$

One can see that if nodes n_1 and n_2 have identical states at $t = t_1$, where $n_1 \geq 2$ and $n_2 \geq 2$, then corresponding $h_n^{(m)}$ are also identical and hence these states remain identical at $t = t_1 + 1$. In the same way any number of subordinates can keep identical states forming a synchronization cluster. Moreover several clusters are also possible.

The existence of the clusters means that the phase space of the considered networks involves corresponding invariant synchronization manifolds. The manifolds can be denoted with sequences of N digits. Zeros represent variables corresponding to non-synchronized nodes, while identical non-zero digits indicate that the corresponding node variables coincide.

The synchronization manifolds have different dimensions and belong to each other forming a hierarchy. There is a single full synchronization manifold encoded with a sequence of N ones $\{111\ldots1\}$. Its dimension is equal to the local dimension of a node oscillator M. This manifold is embraced by $2M$ dimensional manifold of full synchronization of all subordinates without the hub. The sequence denoting it has zero on the first position and $N - 1$ ones: $\{011\ldots1\}$. Then there is a set of $3M$ dimensional manifolds containing clusters where all but one of the subordinates are synchronized. The encoding sequences are: $\{0011\ldots1\}$, $\{0101\ldots1\}$, $\{0110\ldots1\}$, and so on. There are $N - 1$ manifolds of this type. If $N \geq 5$, there are $3M$ dimensional manifolds corresponding to two clusters. These are $\{02211\ldots1\}$, $\{02121\ldots1\}$, $\{02112\ldots1\}$, and so an. The number of such manifolds is $(N-1)!/[i!(N-1-i)!]$, where $2 \leq i \leq N - 3$ is the size of the second cluster. The manifold $\{011\ldots1\}$ is the intersection of all $3M$ dimensional manifolds. The depth of this hierarchy depends on N. On the bottom level there are manifolds of dimension $(N-1)M$ containing clusters of two synchronized subordinates. The encoding sequences are $\{01100\ldots0\}$, $\{00110\ldots0\}$, $\{00011\ldots0\}$, and so on. Figure 2 illustrates this showing the complete hierarchy for $N = 5$.
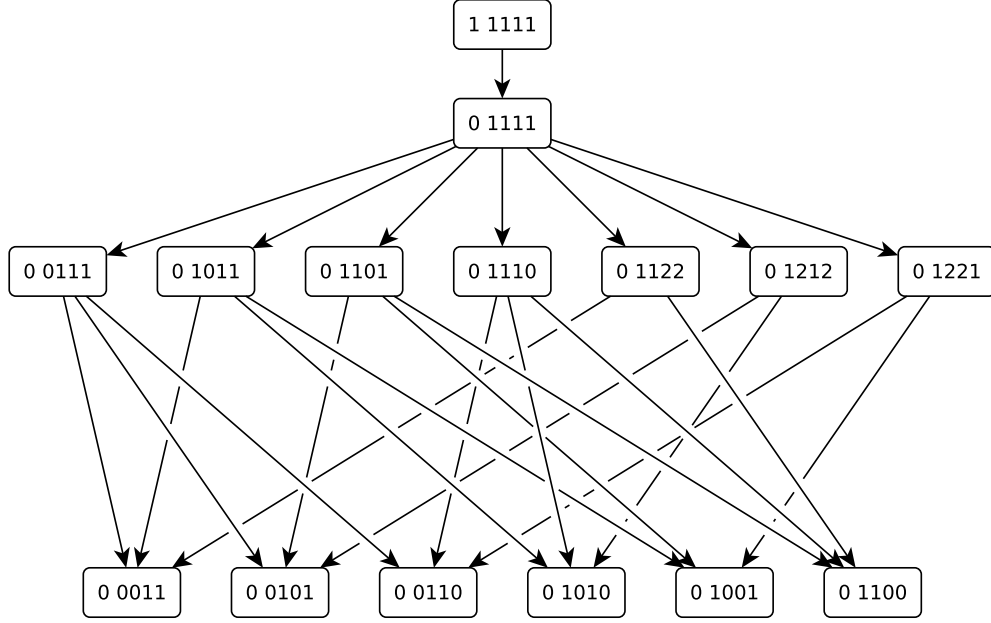
Figure 2. Embedding structure of invariant manifolds for a starlike network of $N = 5$ nodes.

5. GLOBAL MASTER STABILITY FUNCTION FOR FULL SYNCHRONIZATION

The stability of the synchronization manifold $\vec{x}_1 = \cdots = \vec{x}_N = \vec{x}$ can be analyzed using so called master stability function (MSF).[1,7] We have to remind however, that for chaotic dynamics this analysis provides only a necessary condition. Due to the embedded into synchronous chaotic attractor limiting sets whose transverse stability can differ from the average stability of the attractor as a whole, the destruction of the full synchronization can occur even when MSF indicates the stability.[9,10]

At the synchronization manifold elements of $\mathbf{B}_{mi}$ are reduced to diagonal matrices with identical elements:

$$\mathbf{F}_{mi} = f_i^{(m)}\mathbf{I}, \quad \mathbf{\Phi}_m = f_{M+1}^{(m)}\mathbf{I}, \quad \mathbf{G}_{mi} = g_i^{(m)}\mathbf{I}, \tag{13}$$

where

$$f_i^{(m)} \equiv \frac{\partial}{\partial x^{(i)}} f^{(m)}(\vec{x}, 0), \quad f_{M+1}^{(m)} \equiv \frac{\partial}{\partial h} f^{(m)}(\vec{x}, 0), \quad g_i^{(m)} \equiv \frac{\partial}{\partial x^{(i)}} g^{(m)}(\vec{x}). \tag{14}$$

Let $\mathbf{U}$ be a column matrix of eigenvectors of $\mathbf{L}$. Decomposing perturbation vectors $\overrightarrow{\delta x}^{(m)}$ over the eigenvectors $\mathbf{U}$ and taking into account that on the synchronization manifold all matrices $\mathbf{B}_{mi}$ are simultaneously diagonalized by $\mathbf{U}$, one obtains an M dimensional map for perturbations to synchronous attractor:

$$\delta y^{(m)}(t + 1) = \sum_{i=1}^{M} \mu_{mi}(\theta) \delta y^{(i)}(t), \tag{15}$$

where θ is an eigenvalue of $\mathbf{L}$ and

$$\mu_{mi}(\theta) = f_i^{(m)} + \epsilon_m f_{M+1}^{(m)} g_i^{(m)} \theta. \tag{16}$$

The existence of the full synchronization solution means that at least one of the eigenvalues of $\mathbf{L}$ is zero and the corresponding eigenvector contains identical elements. This eigenvector is responsible for longitudinal perturbations to synchronous attractor. All nonzero eigenvalues correspond to transverse perturbations and thus are responsible for average stability of full synchronization.

4

Thus iterating a single local map and computing the first Lyapunov exponents using Eq. (15) one obtains global MSF for the network as $\max\{\lambda_{\text{gmsf}}(\theta) \,|\, \theta > 0\}$, i.e., the synchronization manifold is stable on average if $\lambda_{\text{gmsf}} < 0$ for any nonzero θ.

6. MASTER STABILITY FUNCTION FOR CLUSTER SYNCHRONIZATION

Let a synchronized cluster includes subordinate nodes with indexes $j_1, j_2,\ldots,j_C$, where $j_n \geq 2$, and $C \leq N - 1$ is the cluster size. It means that $\vec{x}_{j_1} = \vec{x}_{j_2} = \cdots = \vec{x}_{j_C}$.

The Jacobian matrix is built of cells $\mathbf{B}_{mi}$ which, in turn, are constructed of diagonal matrices $\mathbf{F}_{mi}$, $\mathbf{\Phi}_{mi}$ and $\mathbf{G}_{mi}$, see Eq. (7) and (10). When the cluster emerges, the corresponding diagonal elements $j_1, j_2,\ldots,j_C$ of these matrices coincides. This results in the coincidence of elements of the first column and the diagonal elements of $\mathbf{B}_{mi}$ with these indexes. The first row of $\mathbf{B}_{mi}$ will contain identical elements multiplied by the corresponding weights w_{j_n}. Let, for example, $N = 5$ and the cluster include three subordinates, $C = 3$: $j_1 = 2$, $j_2 = 3$, and $j_3 = 4$. Then the cell $\mathbf{B}_{mi}$ of the Jacobian matrix has the following structure:

$$\mathbf{B}_{mi} = \begin{pmatrix} b_{mi11} & w_2 q_{mi} & w_3 q_{mi} & w_4 q_{mi} & b_{mi15} \\ r_{mi} & p_{mi} & 0 & 0 & 0 \\ r_{mi} & 0 & p_{mi} & 0 & 0 \\ r_{mi} & 0 & 0 & p_{mi} & 0 \\ b_{mi51} & 0 & 0 & 0 & b_{mi55} \end{pmatrix} \tag{17}$$

To verify stability of the cluster we have to consider the evolution of transverse tangent perturbations to its trajectories. Consider a perturbation vector represented in block form as $\overrightarrow{\delta x}_\perp = \left(\overrightarrow{\delta x}^{(1)}, \overrightarrow{\delta x}^{(2)}, \ldots, \overrightarrow{\delta x}^{(M)}\right)^{\text{T}}$. Each element of this vector has zeros everywhere except for the sites $j_1, j_2,\ldots,j_C$ corresponding to the cluster:

$$\overrightarrow{\delta x}^{(i)} = \left(\ldots, 0, \delta x^{(i)}_{j_1}, \delta x^{(i)}_{j_2}, \ldots, \delta x^{(i)}_{j_C}, 0, \ldots\right) \tag{18}$$

Moreover, the following holds:

$$\sum_{n=1}^{C} w_{j_n} \delta x^{(i)}_{j_n} = 0. \tag{19}$$

One can easily check that $\overrightarrow{\delta x}^{(i)}$ given by Eqs. (18), and (19) is an eigenvector of $\mathbf{B}_{mi}$ with the eigenvalue p_{mi}:

$$\mathbf{B}_{mi}\overrightarrow{\delta x}^{(i)} = \overrightarrow{\delta x}^{(i)} p_{mi}. \tag{20}$$

In view of these properties the evolution of the tangent vectors $\overrightarrow{\delta x}_\perp$ is described as follows:

$$\overrightarrow{\delta x}^{(m)}(t + 1) = \sum_{i=1}^{M} \mathbf{B}_{mi} \overrightarrow{\delta x}^{(i)}(t) = \sum_{i=1}^{M} p_{mi}\overrightarrow{\delta x}^{(i)}(t). \tag{21}$$

Thus, the Jacobian matrix $\mathbf{J}$ acts on transverse perturbation vector $\overrightarrow{\delta x}_\perp(t)$ in the same ways as a block matrix $\mathbf{J}'$ build of $M \times M$ diagonal cells $\mathbf{B}'_{mi}$ with identical diagonal elements:

$$\mathbf{B}'_{mi} = p_{mi}\mathbf{I}. \tag{22}$$

To conclude if the cluster is stable, we need to compute Lyapunov exponent corresponding to the perturbation vector $\overrightarrow{\delta x}_\perp(t)$. In course of the computations we first normalize $\overrightarrow{\delta x}_\perp(t)$, make a step with the Jacobian matrix as defined by Eq. (21) and find a norm of the resulting vector $\overrightarrow{\delta x}^{(m)}(t + 1)$ which is

$$\left\|\overrightarrow{\delta x}_\perp(t + 1)\right\|^2 = \sum_{i,j,m} p_{mi} p_{mj} \left[\overrightarrow{\delta x}^{(j)}(t)\right]^{\text{T}} \overrightarrow{\delta x}^{(i)}(t). \tag{23}$$

5

Lyapunov exponent is an average logarithms of these norms. Important is that the norm does not depend on the number of nodes N. Moreover, the theory of Lyapunov exponents establishes that they do not depend on the choice of the initial vector $\vec{\delta x}_\perp(0)$.[11] Thus, to check the transverse stability of the cluster, it is enough to iterate matrices $\mathbf{P} = \{p_{mi}\}$ with non-block tangent vector of M elements periodically performing its re-normalization,

$$\delta x^{(m)}(t+1) = \sum_{i=1}^{M} p_{mi} \delta x^{(i)}(t).\tag{24}$$

We will refer the Lyapunov exponent, computed as average logarithm of norms of this vector as a cluster master stability function (CMSF). Elements of $\mathbf{P}$ are taken from the matrix (10) where elements are defined by Eqs. (7).

$$p_{mi} = \frac{\partial f^{(m)}}{\partial x^{(i)}}(\vec{x}, h^{(m)}) - \epsilon_m \frac{\partial f^{(m)}}{\partial h}(\vec{x}, h^{(m)}) \frac{\partial g^{(m)}}{\partial x^{(i)}}(\vec{x}).\tag{25}$$

Here $\vec{x}$ and $h^{(m)}$ is computed at the corresponding synchronization cluster.

7. CLUSTER RELATED NETWORK REDUCTION

Since any cluster belongs to an invariant manifold, theoretically, initially identical variables corresponding to the cluster have to be identical forever, i.e., $\vec{x}_{j_1}(t) = \vec{x}_{j_2}(t) = \cdots = \vec{x}_{j_C}(t)$ for any t. It is well known, however, that in actual computations this may not be the case. When the synchronization cluster is transversely unstable an unavoidable numerical noise due to round-off errors destroys it. Nevertheless the deviation from the invariant manifold afthe er one time step is small. Thus, to compute $\vec{x}$ and $h^{(m)}$ for CMSF of a given cluster one can correct this deviation at each step by assigning to cluster variables identical values equal to their average.

Being the most simple and straightforward this method is not the optimal since requires redundant computations. One can instead iterate a reduced network where a set of cluster nodes with identical states is represented by a single node. The weight of this node link is equal to the sum of weights of initial nodes belonging to the cluster.

Figure 3 illustrates the reduction of the star with $N = 5$ and weights $w_2 = 3$, $w_3 = 2$, $w_4 = 1$, $w_5 = 1$. If the nodes 2, 3 and 4 get synchronized, the network dynamics will be reproduced by the reduced network with $N = 3$. The node 2 of this new network represents the cluster having the weight $w'_2 = w_2 + w_3 + w_4$.

To understand why this reduction is possible, consider $h_1^{(m)}$ for the original network, shown in Fig. 3:

$$h_1^{(m)} = \epsilon_m \left\{ \left[3g^{(m)}(\vec{x}_2) + 2g^{(m)}(\vec{x}_3) + g^{(m)}(\vec{x}_4) + g^{(m)}(\vec{x}_5) \right]/7 - g^{(m)}(\vec{x}_1) \right\}.\tag{26}$$

When the nodes 2, 3 and 4 are synchronized, $g^{(m)}(\vec{x}_2) = g^{(m)}(\vec{x}_3) = g^{(m)}(\vec{x}_4)$ and $h_1^{(m)}$ reads:

$$h_1^{(m)} = \epsilon_m \left\{ \left[6g^{(m)}(\vec{x}_2) + g^{(m)}(\vec{x}_5) \right]/7 - g^{(m)}(\vec{x}_1) \right\}.\tag{27}$$

Since $h_n^{(m)}$ with $n \geq 2$ are given by Eq. (12) regardless of N and w_j, one can reproduce the dynamics in presence of the cluster by substituting the three original nodes with the one whose link has weight 6.

In some cases one more reduction step can be made. Consider, for example, the network of $N = 5$ nodes with weights $w_2 = w_3 = w_4 = w_5 = 1$. Let there are two clusters such that subordinate nodes get synchronized pairwise: 2nd with 3rd and 4th with 5th. This network is reduced to the network with $N = 3$ nodes whose link have weights $w_2 = w_3 = 2$. Now since the coupling is normalized so that each $h_n^{(m)}$ with $n \geq 2$ is always given by Eq. (12), the original synchronous dynamics will be reproduced by the network with $N = 3$ and weights $w_2 = w_3 = 1$.

This can be treated in reciprocal order: Each starlike network with integer positive weights correspond to a larger network some of whose nodes are synchronized.
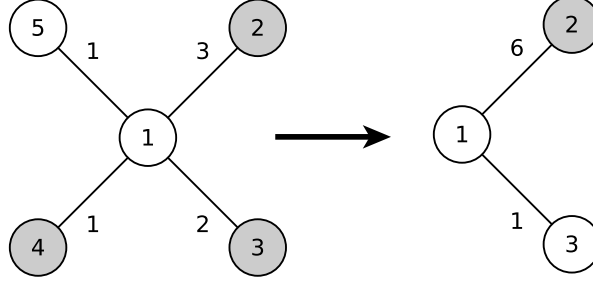
Figure 3. Reduction of a starlike network. If the nodes 2, 3, and 4 get synchronized they can be changed with the single node whose link weight is 6.

8. EXAMPLES

8.1 Ikeda starlike network

This map was suggested by Ikeda[12] and Ikeda et al.[13] We build a starlike network of Ikeda maps and introduce the coupling between the nodes of Ikeda network using ideas reported by Otsuka and Ikeda[14] and by Otsuka et al.:[15]

$$z_n(t+1) = \alpha + \beta w[z_n(t)] + \epsilon \left(\sum_{j=1}^{N} \frac{a_{nj}}{k_n} w[z_j(t)] - w[z_n(t)] \right), \qquad (28)$$

where $z_n(t)$ is a complex variable and $w(z) = z e^{i(|z|^2 + \phi)}$. In what follows the parameters of this system will be $\alpha = 2$, $\beta = 0.5$, $\phi = 0.3$. For these values a single uncoupled system demonstrates chaos with the Lyapunov exponents $\lambda_1 = 0.868$, $\lambda_2 = -2.254$.

As discussed by Kuptsov and Kupstova,[6] the phase space of a starlike network can contain spuriously stable limit sets. They emerge due to round-off errors in computations. To eliminate them, a very small noise of the amplitude 10^{-12} will be added to variables at each step. This noise is found to be too small to result in any observable changes of the dynamics, however it is enough to eliminate spurious regimes.

For the Ikeda network the generalized model (1), (2) takes a form: $f^{(1)}(\vec{x}, h) = \alpha + \beta u(x^{(1)}, x^{(2)}) + h$, $f^{(2)}(\vec{x}, h) = \beta v(x^{(1)}, x^{(2)}) + h$, $g^{(1)}(\vec{x}) = u(x^{(1)}, x^{(2)})$, $g^{(2)}(\vec{x}) = v(x^{(1)}, x^{(2)})$, where $u(x^{(1)}, x^{(2)}) = x^{(1)} \cos \theta - x^{(2)} \sin \theta$, $v(x^{(1)}, x^{(2)}) = x^{(1)} \sin \theta + x^{(2)} \cos \theta$, $\theta = (x^{(1)})^2 + (x^{(2)})^2 + \phi$, $\epsilon_1 = \epsilon_2 = \epsilon$.

According to the results reported by Kuptsov and Kupstova,[6] starlike networks can demonstrate very rich multistability. To distinguish various regimes emerging and vanishing as the coupling strength changes, we will use the first Lyapunov exponent. Being positive, it indicates the presence of chaos; the negative sign reveals periodicity; and the zero signals quasi-periodicity. It is very unlikely (though, of course, not totally excluded) that different regimes will have identical Lyapunov exponents. Thus, to reveal a sort of dynamics we will take a pool of random initial conditions and compute λ_1 for each corresponding trajectory. Grouping of the resulting values near a few point indicates the presence of multiple regimes. This approach is often used for analysis of multistability.[5, 6]

Figure 4(a) shows the first Lyapunov exponent of the Ikeda network with $N = 5$ and unit weights of links computed for various initial conditions vs. ϵ. One can observe that chaotic regimes dominate, but also there are areas where dynamics is periodic. Many different λ_1 at the same ϵ reveals multistability.
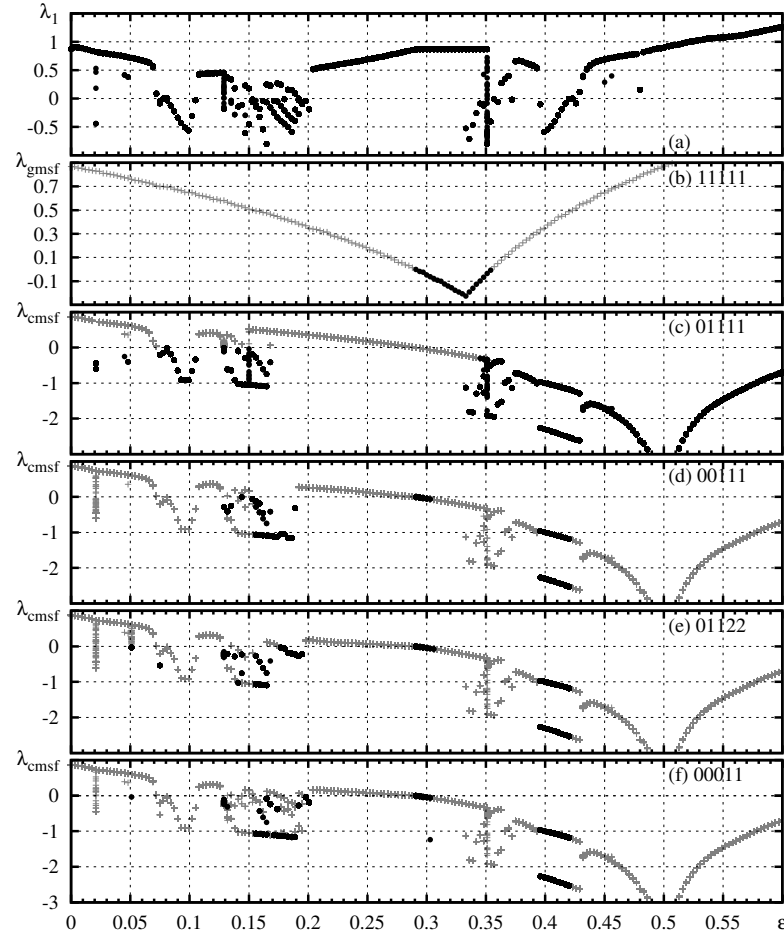
7

Figure 4. Regimes of Ikeda starlike network (28) and their stability: the first Lyapunov exponent λ_1 (a), global MSF (b) and CMSF (c,d,e,f) for all possible clusters admitted at $N = 5$.

Figure 4(b) shows the global MSF computed as described in Sec 5. Solid bullet points mark negative λ_{gmsf}, while gray crosses represent positive ones. The area of stability is

$$0.288 < \epsilon < 0.357. \tag{29}$$

These boundaries are determined from the straightforward inspection of the data computed for Fig. 4(b). The precision is 0.003. Obviously, one can compute them more precisely, however this sufficiently low precision is enough for us.

Figures 4(c,d,e,f) represent CMSFs for all clusters admitted at $N = 5$. The figure legends contains encoding sequences labeling corresponding invariant manifold in the same way as in Fig. 2. Black bullet point is plotted when the corresponding cluster is stable, $\lambda_{\text{cmsf}} < 0$, and other types of synchronization are absent, i.e., we are outside of the embracing synchronization manifold, see the discussion in Sec. 4. Otherwise gray crosses are plotted.

Within the area given by inequalities (29) the full synchronization regime is expected to be observed, since it is transversally stable on average. However, as we already mentioned above, this is the case only for regular dynamics, while for full chaotic synchronization global MSF is necessary but not sufficient condition.

Comparing Figs. 4(a) and (b) we observe that the left boundary of the stability of the global synchronization regime in Fig. 4(a) very well coincides with the predicted one via MSF. (One can easily distinguishes the regime of the full chaotic synchronization in Fig. 4(a) as a horizontal line at level of λ_1 coinciding with λ_1 for uncoupled maps at $\epsilon = 0$.) However at the right edge the full synchronization disappears earlier. First, one can see in Fig. 4(b) that the cluster $\{01111\}$ becomes stable already at $\epsilon = 0.33$. This results in the multistability when this cluster coexists with the full synchronization. An illustration of this regime is shown in Fig. 5(c). At $\epsilon = 0.35$ Lyapunov exponents in Fig. 4(a) are arranged along a straight line ranging approximately from -1 to 1. The most reasonable explanation of this volatility is the presence of called unstable dimension variability (UDV).[16] It is known that typically on the edges of stability of full synchronization regimes there are a lot of periodic orbits with different dimensions of unstable manifold. The trajectory passes in vicinities of these orbits changing its own unstable manifold dimension. In particular it results in very bad convergence of Lyapunov exponents.

Moving further to the right outside of the range (29) we observe in Fig. 4(c) the presence of multistability of regimes with fully synchronized subordinate nodes. They can be both chaotic and regular.

The area $0.39 < \epsilon 0.42$ is highlighted by black bullet points simultaneously in all Figs 4(c,d,e,f). This is a specific reaction of the computation algorithm to so called oscillation death that takes place here. All nodes do not oscillate, the subordinate stay in one point and the hub has another state. Notice two values of λ_{cmsf} here. They correspond to the interchange of the states of the hub and the subordinates.

Further to the right the cluster with synchronized subordinate nodes remain the only stable regime, see black bullet points in Fig. 4(c) at $\epsilon > 0.42$.

On the left edge of the synchronization area, at approximately $0.29 < \epsilon \approx 0.3$ Figs. 4(d,e,f) indicate simultaneous stability of clusters with three or two nodes. However no multistability is registered in Fig. 4(a). More detailed inspection reveals that here is an area of intermittency. Nodes get almost synchronized for some time, but then a desynchronization occurs. An example of this behavior is shown in Fig. 5(b).

To the left of the full synchronization area (29) we observe first a chaotic regime without multistability, see Fig. 4(a). The gray crosses on on the panels below, Fig. 4(b,c,d,e,f) indicate that no synchronization clusters can happen here.

Below $\epsilon = 0.2$ there is an area of multistability. Fig. 4(a) shows here a variety of regimes, both chaotic and regular. Black bullet points in Figs. 4(d,e,f) indicate that this multistability is related with the presence of synchronization clusters of different types. The emergence of the rich multistability area below the full synchronization regime was already reported by Kuptsov and Kuptsova for a starlike network of Hénon maps.[6] An example of dynamics in this area is shown in Fig. 5(a).
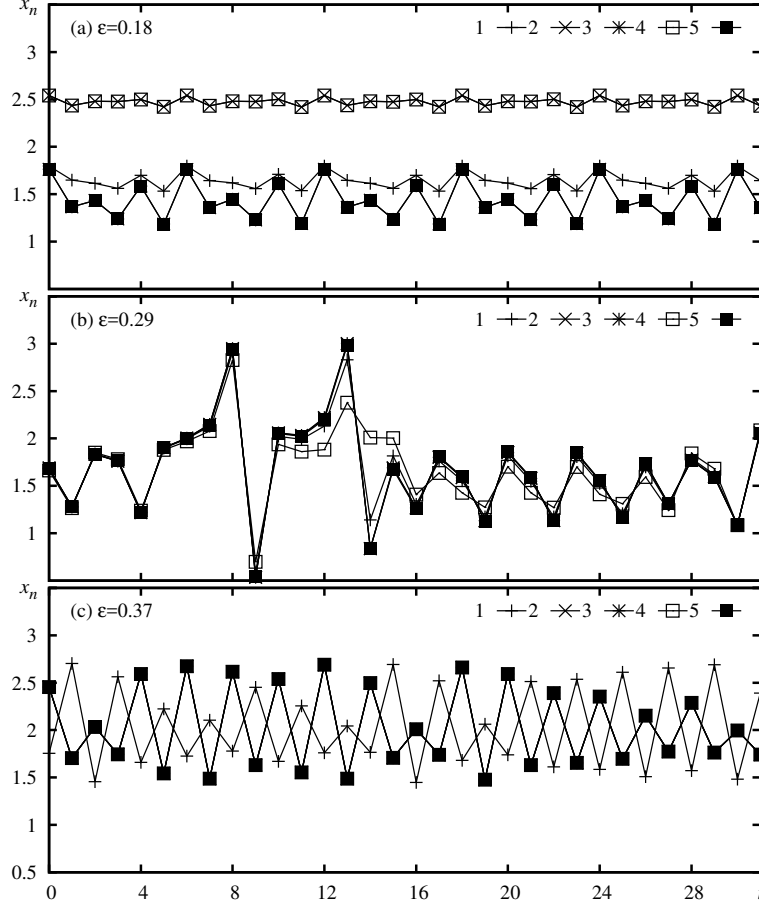
9

Figure 5. Time series of Ikeda starlike network (28).

8.2 Predator-prey starlike network

The predator-prey network can be built analogously to a lattice of predator-prey maps considered by Solé and Valls:[17]

$$x_n(t+1) = \alpha x_n(t)[1 - x_n(t) - y_n(t)] + \epsilon \left(\sum_{j=1}^{N} \frac{a_{nj}}{k_n} x_j(t) - x_n(t) \right),$$

$$y_n(t+1) = \beta x_n(t) y_n(t) + d\epsilon \left(\sum_{j=1}^{N} \frac{a_{nj}}{k_n} y_j(t) - y_n(t) \right). \tag{30}$$

Again a very small noise of the amplitude 10^{-12} is added at each step to destroy spurious regimes. The generalized model (1), (2) for this network reads: $f^{(1)}(\vec{x}, h) = \alpha x^{(1)}(1 - x^{(1)} - x^{(2)} + h$, $f^{(2)}(\vec{x}, h) = \beta x^{(1)} x^{(2)} + h$, $g^{(1)}(\vec{x}) = x^{(1)}$, $g^{(2)}(\vec{x}) = x^{(2)}$, and $\epsilon_1 = \epsilon$, $\epsilon_2 = d\epsilon$.

The first Lyapunov exponent as well as master stability functions are shown in Fig. 6. First of all notice that there are two areas where the whole network can be stable, see Fig. 6(a). Their boundaries are

$$0.235 < \epsilon < 0.380, \quad 0.540 < \epsilon. \tag{31}$$

The oscillations of the network diverges at $\epsilon > 0.6$.

The multistability is observed almost everywhere, except for the right full synchronization area. Within the left area there is the second attractor which is quasiperiodic, since its λ_1 vanishes. Also at $\epsilon > 0.28$ more
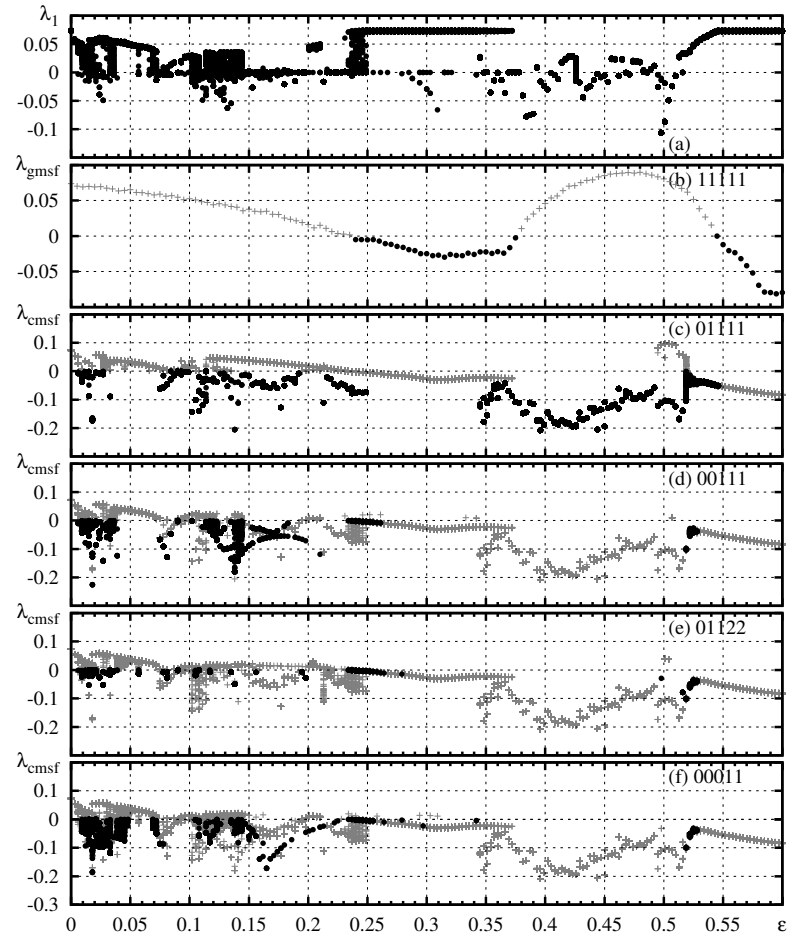
10

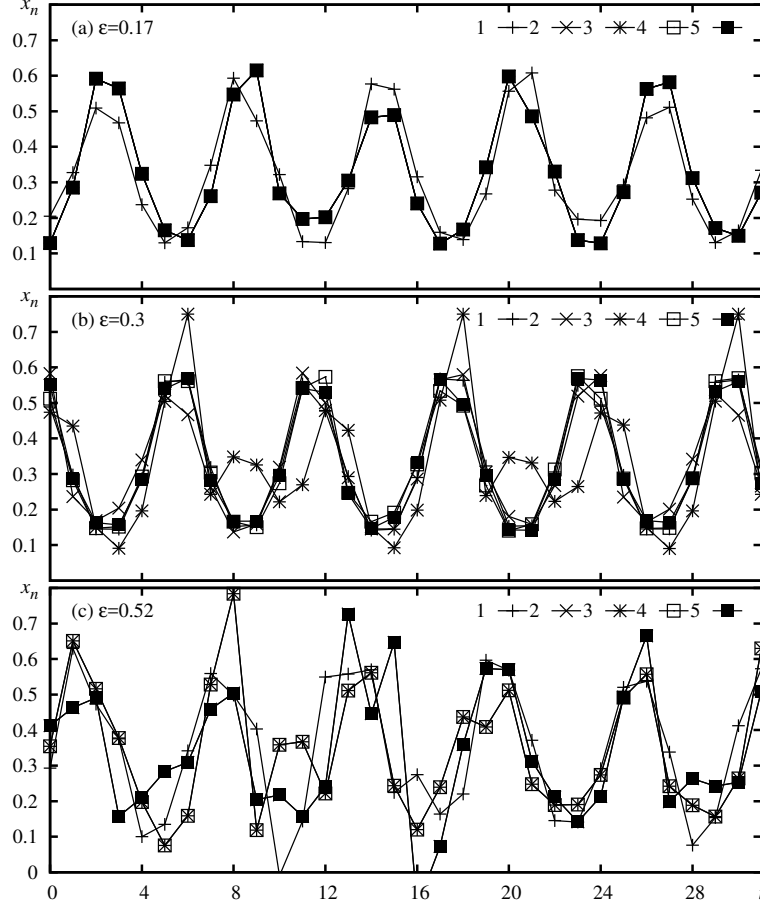Figure 6. Same as Fig. 4 for predator-prey starlike network (30), $N = 5$.

Figure 7. Time series of predator-prey starlike network (30).

attractors coexist with the full synchronization, both chaotic ($\lambda_1 > 0$) and periodic ($\lambda_1 < 0$). An example of chaotic dynamics here is shown in Fig. 7(b).

To the right of the first full synchronization area the cluster {01111} becomes stable as above for the Ikeda network. Near the second area we again observe multistability, see points around $\epsilon = 0.52$ in Figs. 6(c,d,e,f). All sorts of clusters can be stable here and the inspection of time series revels that corresponding regimes can indeed be observed. For example, Fig. 7(c) shows chaotic oscillations with synchronized 2nd and 5th nodes as well as 3rd and 4th ones.

To the left of the first full synchronization area we again observe rich multistability. Figures 6(c,d,e,f) demonstrates that all sorts of clusters can emerge here. An illustration of the dynamics is shown in Fig. 7(a).

The specific feature of the discussed network is high volatility of the first Lyapunov exponent at $\epsilon < 0.25$, see Fig. 6(a). Instead of grouping around several points almost continues ranges of values are observed. We address it to the rich multistability and UDP related to it. Phase space is filled up with interwoven limiting sets with different numbers of unstable manifolds. Since a trajectory passes around these sets its unstable manifold dimension fluctuates so that the convergence of the first Lyapunov exponent becomes very bad.

12

8.3 Hénon starlike network

Starlike network of Hénon maps can be built as generalization of the Hénon chain suggested by Politi and Torcini:[18]

$$x_n(t+1) = \alpha - \left[x_n(t) + \epsilon \left(\sum_{j=1}^{N} \frac{a_{nj}}{k_n} x_j(t) - x_n(t) \right) \right]^2 + y_n(t),$$

$$y_n(t+1) = \beta x_n(t),$$

$$(32)$$

Here $\alpha = 1.4$ and $\beta = 0.3$ are the parameters controlling local dynamics. Recall that the Hénon map is time-reversible. The coupling is introduced in a way that preserves this property. As for previous networks we add very small noise with the amplitude 10^{-12} to destroy spurious regimes. The general form (1), (2) for this map reads: $f^{(1)}(\vec{x}, h) = \alpha - (x^{(1)} + h)^2 + x^{(2)}$, $f^{(2)}(\vec{x}, h) = \beta x^{(1)}$, $g^{(1)}(\vec{x}) = x^{(1)}$, $g^{(2)}(\vec{x}) = 0$, and $\epsilon_1 = \epsilon$, $\epsilon_2 = 0$.

We already considered starlike network of Hénon maps in detail.[6] In particular time series of all regimes were presented and discussed. Thus, in the present paper we show only the first Lyapunov exponent, Fig. 8(a), compared with both the global MSF and CMSFs, Fig. 8(b) and Fig. 8(c,d,e,f), respectively.

As for two previous networks we observe the area where the full synchronization attractor can be stable. It lays within the range

$$0.348 < \epsilon < 0.826. \tag{33}$$

Notice that the overall picture of dynamics is qualitatively similar to that for Ikeda map discussed in Sec. 8.1. To the right of the area of the full synchronization there is an area of oscillation death, $0.8 < \epsilon < 0.83$. It manifests itself as black bullet points emerging simultaneously on panels (c), (d), (e) and (f). More to the right the cluster {01111} becomes stable, see Fig. 8(c). To the left of the area of full synchronization we have an intermittency, see bars of black bullet points in Figs. 8(d,e,f) at $0.34 < \epsilon 0.38$. Then to the left of this regime we observe chaotic oscillations at $0.26 < \epsilon < 0.34$. And further to the left we encounter multistability. Here all clusters can be stable, but the cluster of all subordinates dominates.

9. CONCLUSION

We considered a generalized model of a starlike network with discrete time oscillators and normalized Laplacian coupling. The coupling admits both full synchronization and cluster synchronization of subordinate nodes. We suggested a necessary condition of stability of clusters. This approach generalizes the well known method of master stability function developed for analysis of full synchronization.

Three networks are considered and the stability of clusters is analyzed. The common feature specific to these three systems is that the area of full synchronization on the axis of the coupling strengths is surrounded by areas where clusters of synchronized subordinates are stable. Within these area very rich multistability is observed.

REFERENCES

[1] Boccaletti, S., Latora, V., Moreno, Y., Chavez, M., and Hwang, D.-U., "Complex networks: Structure and dynamics," *Physics Reports* **424**(4–5), 175 – 308 (2006).

[2] Wang, X. F., "Complex networks: topology, dynamics and synchronization," *International Journal of Bifurcation and Chaos* **12**(05), 885–916 (2002).

[3] Barabási, A.-L., Albert, R., and Jeong, H., "Scale-free characteristics of random networks: the topology of the world-wide web," *Physica A* **281**(1–4), 69 – 77 (2000).

[4] Feudel, U., "Complex dynamics in multistable systems," *International Journal of Bifurcation and Chaos* **18**(06), 1607–1626 (2008).
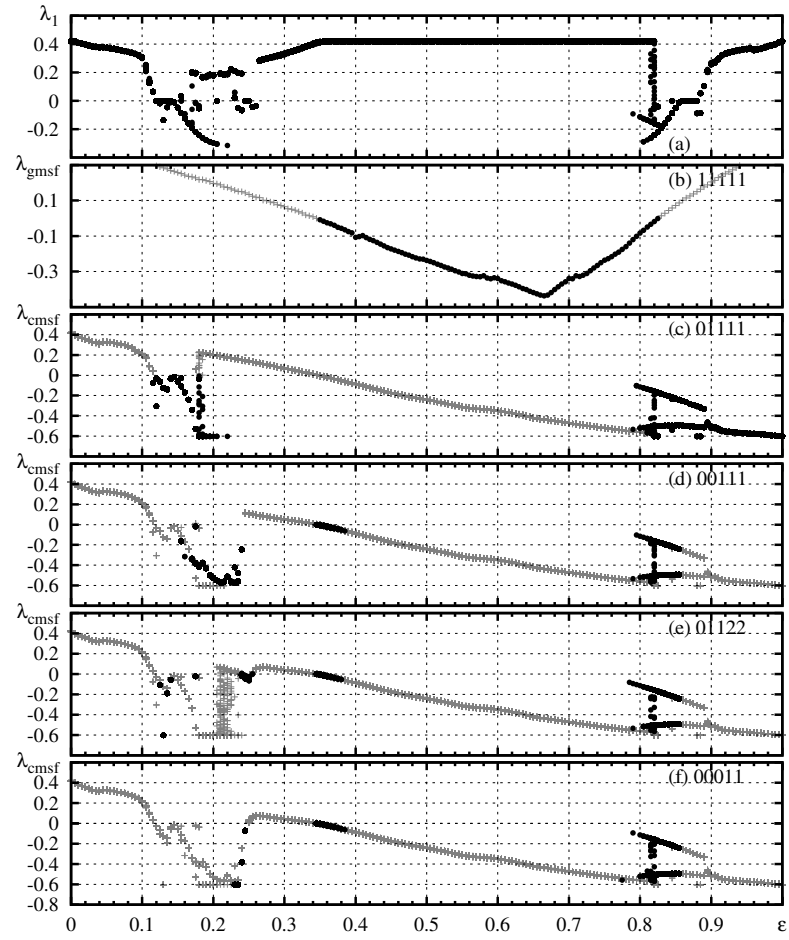
Figure 8. Same as Fig. 4 for Hénon starlike network (32), $N = 5$.

[5] Pisarchik, A. N. and Feudel, U., "Control of multistability," *Physics Reports* **540**(4), 167 – 218 (2014). Control of multistability.

[6] Kuptsov, P. V. and Kuptsova, A. V., "Variety of regimes of starlike networks of hénon maps," *Phys. Rev. E* **92**, 042912 (Oct 2015).

[7] Pecora, L. M. and Carroll, T. L., "Master stability functions for synchronized coupled systems," *Phys. Rev. Lett.* **80**, 2109–2112 (Mar 1998).

[8] Kuptsov, P. V. and Kuptsova, A. V., "Predictable nonwandering localization of covariant lyapunov vectors and cluster synchronization in scale-free networks of chaotic maps," *Phys. Rev. E* **90**, 032901 (Sep 2014).

[9] Milnor, J., "On the concept of attractor," in [*The Theory of Chaotic Attractors*], 243–264, Springer (2004).

[10] Ott, E. and Sommerer, J. C., "Blowout bifurcations: the occurrence of riddled basins and on-off intermittency," *Physics Letters A* **188**(1), 39 – 47 (1994).

[11] Kuptsov, P. V. and Parlitz, U., "Theory and computation of covariant Lyapunov vectors," *J. Nonlinear Sci.* **22**(5), 727–762 (2012).

[12] Ikeda, K., "Multiple-valued stationary state and its instability of the transmitted light by a ring cavity system," *Optics Communications* **30**(2), 257 – 261 (1979).

[13] Ikeda, K., Daido, H., and Akimoto, O., "Optical turbulence: Chaotic behavior of transmitted light from a ring cavity," *Phys. Rev. Lett.* **45**, 709–712 (Sep 1980).

[14] Otsuka, K. and Ikeda, K., "Hierarchical multistability and cooperative flip-flop operation in a bistable optical system with distributed nonlinear elements," *Optics letters* **12**(8), 599–601 (1987).

[15] Otsuka, K. and Ikeda, K., "Self-induced spatial disorder in a nonlinear optical system," *Phys. Rev. Lett.* **59**, 194–197 (Jul 1987).

[16] Kostelich, E. J., Kan, I., Grebogi, C., Ott, E., and Yorke, J. A., "Unstable dimension variability: A source of nonhyperbolicity in chaotic systems," *Physica D: Nonlinear Phenomena* **109**(1–2), 81 – 90 (1997). Proceedings of the Workshop on Physics and Dynamics between Chaos, Order, and Noise.

[17] Solé, R. V. and Valls, J., "Order and chaos in a 2d lotka-volterra coupled map lattice," *Physics Letters A* **153**(6), 330–336 (1991).

[18] Politi, A. and Torcini, A., "Periodic orbits in coupled Hénon maps: Lyapunov and multifractal analysis," *Chaos* **2**, 293–300 (1992).